Scaling of dynamic spin correlations in $BaCu_2(Si_{0.5}Ge_{0.5})_2O_7$

A. Zheludev
HFIR Center for Neutron Scattering, Oak Ridge National Laboratory, Oak Ridge, Tennessee 37831-6393, USA

T. Masuda
International Graduate School of Arts and Sciences, Yokohama City University, 22-2, Seto, Kanazawa-ku, Yokohama City, Kanagawa 236-0027, Japan

G. Dhalenne and A. Revcolevschi
Laboratoire de Physico-Chimie de l'Etat Solide, Universite Paris-Sud, 91405 Orsay Cedex, France

C. Frost and T. Perring
ISIS Facility, Rutherford Appleton Laboratory, Chilton, Didcot, Oxfordshire OX11 0QX, UK
(Received 1 November 2006; published 13 February 2007)

The magnetic dynamic structure factor of the one-dimensional $S=1/2$ chain system $BaCu_2(Si_{0.5}Ge_{0.5})_2O_7$ is studied in a wide range of energy transfers and temperatures. Contrary to previous erroneous reports [T. Masuda *et al.*, Phys. Rev. Lett. **93**, 077206 (2004)], the scaling properties observed in the range 0.5–25 meV are found to be fully consistent with expectations for a Luttinger spin liquid. At higher energies, a breakdown of scaling laws is observed and attributed to lattice effects. The results are complementary to those found in literature for other $S=1/2$ chain compounds, such as $KCuF_3$ and Cu benzoate.

DOI: 10.1103/PhysRevB.75.054409 PACS number(s): 75.40.Gb, 75.10.Jm, 75.50.Ee

I. INTRODUCTION

The two isostructural oxides $BaCu_2Ge_2O_7$ and $BaCu_2Si_2O_7$ are prototypical quasi-one-dimensional quantum $S=1/2$ antiferromagnets (AFs).[1] Previous extensive neutron-scattering experiments on $BaCu_2Si_2O_7$ were instrumental in developing an understanding of the spin dynamics in weakly coupled $S=1/2$ chains.[2–5] More recently, solid solutions of type $BaCu_2(Si_{1-x}Ge_x)_2O_7$ were recognized as potential spin chain systems with random bond strengths.[6] Bulk measurements[6–8] and preliminary neutron-scattering studies[6] indicated that the $x=0.5$ compound shows some very unusual scaling of the static magnetic susceptibility and the dynamic spin-correlation function. It was proposed that due to an intrinsic quenched structural disorder, $BaCu_2(Si_{0.5}Ge_{0.5})_2O_7$ is an experimental realization of the much-studied random singlet model[9,10] and shows scaling properties predicted by Damle *et al.*[11,12] Unfortunately, when follow-up measurements were performed on larger and higher quality samples, these conclusions were shown to be erroneous.[13] In fact, in a wide energy range, the magnetic dynamic structure factor $S(q,\omega)$ follows theoretical expectations for disorder-free spin chains. In the present paper, we report detailed temperature-dependent measurements of magnetic excitations in $BaCu_2(Si_{0.5}Ge_{0.5})_2O_7$ obtained using the large single-crystal samples. The focus is on scaling relations for the spin-correlation function. Convenient magnitudes of magnetic interactions enable us to cover a wide dynamic range $\hbar\omega/\kappa T \approx 1-100$. In this work, our results are complementary to those previously obtained for two other $S=1/2$ chain systems, namely, Cu benzoate[14] and $KCuF_3$ (Ref. 15), where $\hbar\omega/\kappa T \approx 0.1-10$.

$BaCu_2(Si_{1-x}Ge_x)_2O_7$ crystallizes in an orthorhombic structure, with space group *Pnma*. The lattice constants linearly depend on the Ge content, and for $x=0.5$, are $a=6.917(7)$ Å, $b=13.28$ Å,[7] and $c=6.944(7)$ Å. Magnetic properties are due to Cu^{2+} ions that form weakly coupled antiferromagnetic chains running along the crystallographic c axis. The in-chain exchange constant is $J=24$ meV for the silicate ($x=0$) and $J=50$ meV for the Ge system ($x=1$).[1] The average coupling strength $\langle J\rangle$ for intermediate concentrations can be deduced from the position of the Bonner-Fisher susceptibility maximum. It increases linearly with x,[7,8] and for $BaCu_2(Si_{0.5}Ge_{0.5})_2O_7$, $\langle J\rangle=37$ meV. The corresponding Des Cloizeau–Pearson (DCP) zone-boundary energy of magnetic excitations is $\hbar\omega_{ZB}=\pi\langle J\rangle/2=58$ meV.[16] Nearest-neighbor spin-spin separation within the chains is equal to $c/2$, so the one-dimensional (1D) AF zone center $q_\parallel=\pi$ corresponds to $l=1$, where (h,k,l) denotes a vector in crystallographic reciprocal space. Weak interactions between the chains result in long-range AF ordering at $T_N=9.2$ K in the silicate and at $T_N=10$ K in the germanate.[1] However, for intermediate concentrations, the transition temperature is suppressed,[7,8] and for $BaCu_2(Si_{0.5}Ge_{0.5})_2O_7$, it is as low as $T_N=0.7$ K.[17] Previous theoretical and neutron-scattering studies have shown that in weakly-coupled spin chains, three-dimensional effects are totally negligible at energies $\hbar\omega \gtrsim 5\kappa T_N$,[2,18] so that barring any disorder-induced effects, $BaCu_2(Si_{0.5}Ge_{0.5})_2O_7$ can be expected to behave like a good 1D system for $\hbar\omega \gtrsim 0.5$ meV. Comparing this energy to $\hbar\omega_{ZB}$, we see that the material presents a conveniently broad energy range for testing any predicted 1D scaling relations for $S(\mathbf{q},\omega)$ in quantum $S=1/2$ chains.

II. EXPERIMENT

In the present study, we used six $BaCu_2(Si_{0.5}Ge_{0.5})_2O_7$ single crystals of a total mass of 15 g, grown using the float-

ing zone method. Most crystals were twinned in such a way that the a and c axes of the two crystallographic domains were interchanged. Such a growth habit is consistent with $a \approx c$, but complicates the measurements, as it involves the chain axis. Individual crystals were coaligned to form a compound sample with a total effective mosaic of 1.7°. Inelastic neutron-scattering data were collected in two separate series of experiments. Experimental setup 1 employed the HB1 thermal three-axis spectrometer installed at the high-flux isotope reactor at ORNL. The final neutron energy was fixed at 14.7 meV. A pyrolitic graphite (PG) monochromator was used in conjunction with a PG filter installed after the sample. The collimation setup was 48′-40′-40′-240′. The sample was mounted with the (a,c) scattering plane horizontal, making crystallographic wave vectors $(h,0,l)$ accessible for measurements. The sample environment was a standard He-flow cryostat. All data were corrected for the wavelength-dependent efficiency of the beam monitor (due to higher-order beam contamination) and the vertical focal length of the fixed-curvature monochromator. It was, in part, an incorrect application of these corrections that led to erroneous conclusions in Ref. 6. The second series of measurements were performed on the MAPS time-of-flight (TOF) chopper spectrometer installed at the ISIS spallation neutron facility at RAL. Incident energy was fixed at either 50 meV (setup 2) or 100 meV (setup 3). The (a,c) plane of the crystal was mounted parallel to the preferential scattering plane of the instrument. All TOF data were integrated along the b^* crystallographic direction in the range $-1<k<1$. Sample temperature was controlled between 5.5 and 300 K using a closed-cycle refrigerator.

III. RESULTS AND DATA ANALYSIS

A. Three-axis data

In three-axis experiments, the data were collected in constant-E scans. Due to the presence of two sets of crystallographic domains, any scattering at wave vector (h,k,l) is observed simultaneously with that at (l,k,h). A steep dispersion of magnetic excitations along the chains implies that at low-energy transfers, all relevant scattering is concentrated near the 1D AF zone centers, l is odd. For this reason, scans performed at $l=0$ effectively pick up the signal from only one of the two domains. While only half of the sample contributes to scattering, this geometry is optimal for achieving a high wave-vector resolution along the chains. A typical constant-E scan of this type measured using setup 1 at $\hbar\omega=12$ meV is shown in Fig. 1(a). An alternative approach is to restrict data collection to $\mathbf{q}=(h\pm x,k,l\pm x)$, where x is arbitrary and h and l are integers. At these positions, the scattering in both crystallographic domains occurs at wave vectors that are equivalent in the 1D sense. The presence of two domains still has to be carefully taken into account when calculating the spectrometer resolution function. This second approach is the only option of high-energy transfers, where in each domain the scattering is spread out over a wide q range and necessarily interferes with that from the other domain. Constant-E scans collected in this mode are shown in Figs. 1(b) and 1(c). A constant background was subtracted from all three-axis scans shown.

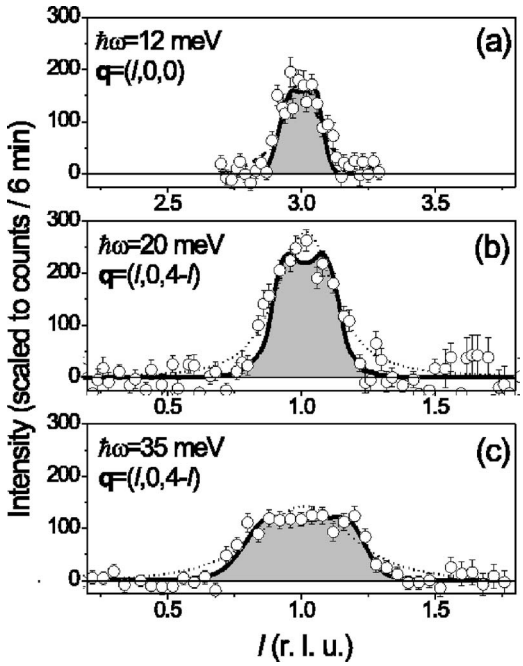

FIG. 1. Constant-E scans measured in $BaCu_2(Si_{0.5}Ge_{0.5})_2O_7$ using setup 1 (three-axis spectrometer) at $T=12$ K (symbols). Heavy solid lines and shaded areas are fits using the Müller ansatz. Dashed lines are Lorentzian fits. All fitting functions are convoluted with the known experimental resolution.

At low temperatures, the magnetic dynamic structure factor of disorder-free quantum $S=1/2$ chains can be accurately approximated by the Müller ansatz[5,15,19–23] (MA). For $BaCu_2(Si_{0.5}Ge_{0.5})_2O_7$, in Ref. 6 it was claimed that in constant-E scans, the magnetic scattering appears broader than the MA expectation and is more consistent with Lorentzian line shapes. It was since realized that the elongated Lorentzian-type "tails" are a result of background contamination.[13] Analyzing these data, we find that the MA peak profiles actually work for $BaCu_2(Si_{0.5}Ge_{0.5})_2O_7$ rather well. For each measured constant-E scan, the MA dynamic structure factor was numerically folded with the known spectrometer resolution function and fitted to the experimental data. The DCP spin-wave velocity v was fixed at $\pi\langle J\rangle c/4 = 404$ meV Å. The only variable parameter was an overall scaling factor. Excellent fits were obtained at all energies (solid lines and shaded areas in Fig. 1). Simulations using Lorentzians convoluted with the experimental resolution function are shown by dashed lines. Lorentzians provide satisfactory fits only at low-energy transfers, where the finer spectral features are masked by the limited experimental resolution anyway. At high energies, deviations from Lorentzian line shapes become obvious, and a flattening at the intensity maximum, resulting in typical "top-hat" shapes, is clearly observed [Fig. 1(c)].

B. TOF data

Specifics of the TOF geometry make separating the signals originating from the two crystallographic domains less

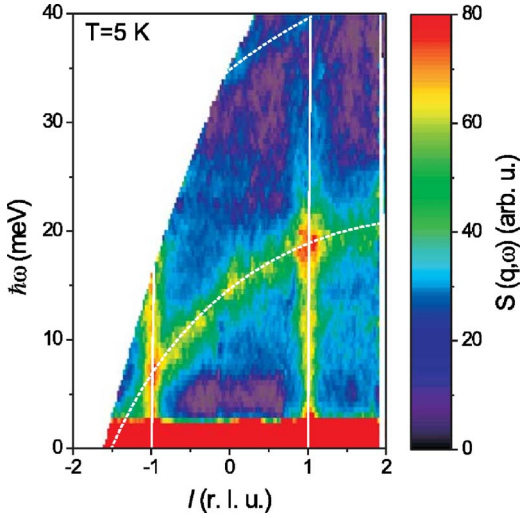

FIG. 2. (Color online) Time-of-flight spectrum collected in $BaCu_2(Si_{0.5}Ge_{0.5})_2O_7$ at $T=5$ K using setup 2, in projection onto the c (chain) axis. Solid and dashed white lines are 1D antiferromagnetic zone centers for the two crystallographic domains present in the sample, respectively.

straightforward. Typical data collected using setups 2 and 3 are shown in Figs. 2 and 3 in the projection onto the c axis of one of the domains (domain A). Vertical streaks of scattering at the 1D AF zone centers, $l=\pm 1$, for this domain are clearly visible and highlighted by vertical solid lines. However, they are intersected by the 1D AF zone centers of the second domain (domain B), represented by the dashed curves. The corresponding magnetic scattering from domain B appears as a series of arcs. In order to separate it from domain-A scattering, one has to rely on certain assumptions and approximations. At small energy transfers, where all the scattering is concentrated in the vicinity of the 1D zone centers, one can simply regard all data collected sufficiently far from domain B 1D zone centers as belonging to domain A. Constant-energy cuts obtained from setup 2 data using this assumption are shown in Fig. 4 (constant background subtracted). Compared to the three-axis data, the experimental wave-vector

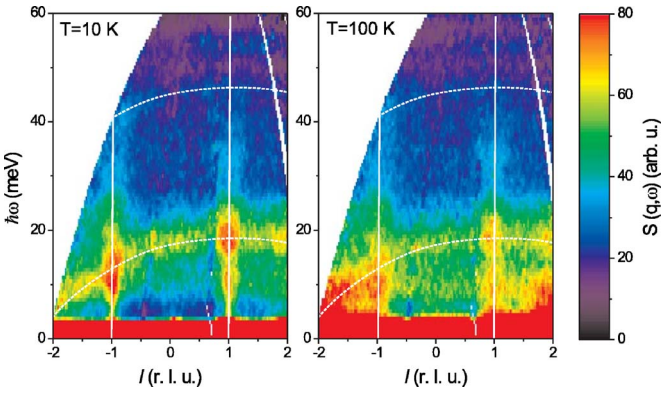

FIG. 3. (Color online) Time-of-flight spectrum collected in $BaCu_2(Si_{0.5}Ge_{0.5})_2O_7$ at $T=5$ K using setup 2, in projection onto the c (chain) axis. Solid and dashed white lines are 1D antiferromagnetic zone centers for the two crystallographic domains present in the sample, respectively.

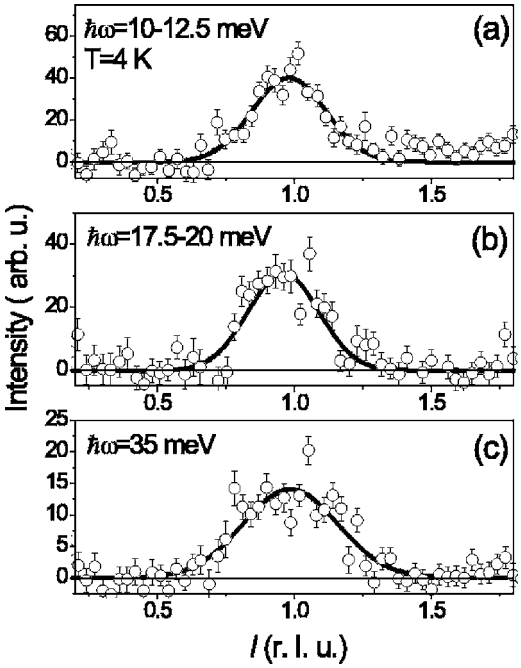

FIG. 4. Typical constant-E cuts of the TOF data for $BaCu_2(Si_{0.5}Ge_{0.5})_2O_7$ collected using setup 2 at $T=4$ K. Solid lines are Gaussian fits. A flat background has been subtracted.

resolution of the TOF setup is insufficient to resolve any fine structure in the scattering profile.

An alternative approach is to select a geometry in which domain-B 1D zone centers cross that of domain A at an almost constant energy, as in the case of $l=1$ in Fig. 3. For a constant-E cut extracted from such a data set, the magnetic scattering by domain B will, to a good approximation, correspond to a constant l value. Since 1D magnetic scattering is independent of h and k, it will amount to a constant background contribution. Constant-energy scans extracted from setup 3 data using this procedure are shown in Fig. 5. A temperature-induced broadening of the scattering profiles is clearly visible. Data analysis at high temperatures is complicated by the increasing phonon contribution to the background [Fig. 3(b) and shaded areas in Fig. 5]. For this reason, the measurements were limited to $T \lesssim 100$ K.

C. Scaling quantities

The central purpose of this study was to investigate the energy and temperature scaling of the spin correlations in $BaCu_2(Si_{0.5}Ge_{0.5})_2O_7$. Much of the existing experimental work concentrated on the scaling of the dynamic structure measured at the 1D zone center, $S(\pi,\omega)$.[14,15] This quantity is defined exclusively by long-wavelength AF spin correlations. In this regime, quantum spin chains are equivalent to a Luttinger spin liquid. The existing exact analytical predictions for this model[24] make a comparison with theory straightforward. The problem, however, is that measuring $S(\pi,\omega)$ requires wave-vector selectivity: the experimental wave-vector resolution δq must be small compared to the q width of scattering at a particular energy transfer. The latter can be estimated as $\hbar\omega/v$, where v is the DCP spin-wave velocity.

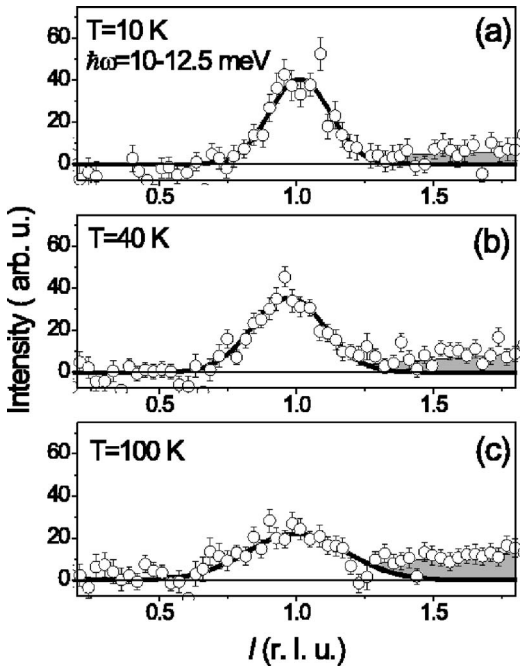

FIG. 5. Temperature evolution of a constant-E cut measured for $BaCu_2(Si_{0.5}Ge_{0.5})_2O_7$ using setup 3. Solid lines are Gaussian fits. A flat background has been subtracted. The shaded area is due to scattering by phonons.

Thus, there will always be a lower limit on energy transfer for the measurements, determined by the experimental resolution: $\hbar\omega_{\min} \sim \delta q v$. This limit is further enforced by the additional complication that the experimental wave-vector resolution changes with energy transfer. For our three-axis setup, the practical lower limit is about 20 meV and is still higher for the TOF experiments. A more robust approach is to measure the q-integrated structure factor $S_0(\omega) = \int S(q,\omega) dq$.[14] In the hydrodynamic limit, the integral is to be taken over the entire q range, but, on a lattice, it should be limited to the vicinity of the 1D AF zone center. Taking the integral entirely eliminates the effect of wave-vector resolution. In our case of $BaCu_2(Si_{0.5}Ge_{0.5})_2O_7$, $S(\omega)$ was determined from the cross-section fits to individual three-axis q scans (solid lines in Fig. 1). For the TOF data, we employed empirical Gaussian fits to constant-E cuts, as shown in solid lines in Figs. 4 and 5. The bulk of the low-temperature data for $S(\omega)$ is shown in Fig. 6 (circles). Reanalyzed data from Ref. 6 are plotted as solid squares (thermal-neutron measurements) and triangles (cold neutrons). The inset shows the same data scaled by the energy transfer. All $S(\omega)$ data collected in this work at different temperatures, after an appropriate scaling (see below), are plotted in Fig. 7. Solid symbols are for energy transfers $\hbar\omega < 25$ meV, while open symbols represent higher energies.

IV. DISCUSSION

The finite-temperature scaling for the dynamic structure factor of a Luttinger spin liquid is given by[24]

$$S(\tilde{q},\omega) \propto (n_\omega + 1)\frac{1}{T}F\left(\frac{\hbar\omega}{\kappa T}, \frac{v\tilde{q}}{\kappa T}\right), \qquad (1)$$

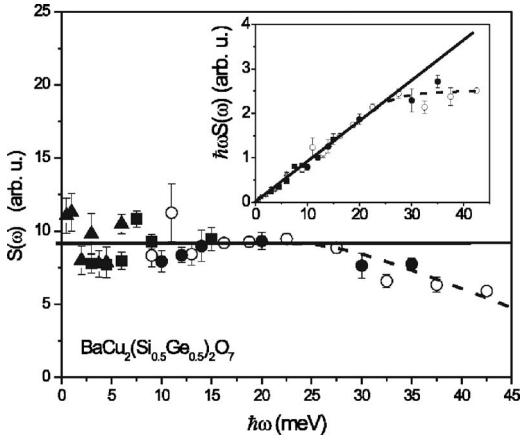

FIG. 6. Scaling of $S(\omega)$ measured in $BaCu_2(Si_{0.5}Ge_{0.5})_2O_7$ (symbols). Solid circles: setup 1 (three-axis), $T=12$ K. Open circles: setup 2 (TOF), $T=5.5$ K. Squares: Ref. 6, reanalyzed thermal-neutron three-axis data, $T=12$ K. Triangles: Ref. 6, cold-neutron three-axis data, $T=1.5$ K. Solid line: Luttinger spin liquid at $T \to 0$. The dashed curves are guides for the eyes. Inset: same plot for $\hbar\omega S(\omega)$.

$$F(x,y) = \mathrm{Im}\left(\frac{\Gamma\left(\frac{1}{4} - i\frac{x-y}{4\pi}\right)}{\Gamma\left(\frac{3}{4} - i\frac{x-y}{4\pi}\right)}\frac{\Gamma\left(\frac{1}{4} - i\frac{x+y}{4\pi}\right)}{\Gamma\left(\frac{3}{4} - i\frac{x+y}{4\pi}\right)}\right), \qquad (2)$$

where $(n_\omega+1) = (1 - e^{-\hbar\omega/(\kappa T)})^{-1}$. For an $S=1/2$ Heisenberg spin chain, this scaling applies to AF spin correlations near a 1D AF zone center $q=q_0$, so that $\tilde{q} = q - q_0$. The integral over $\tilde{q}$ needed to derive the scaling for $S(\omega)$ cannot be easily

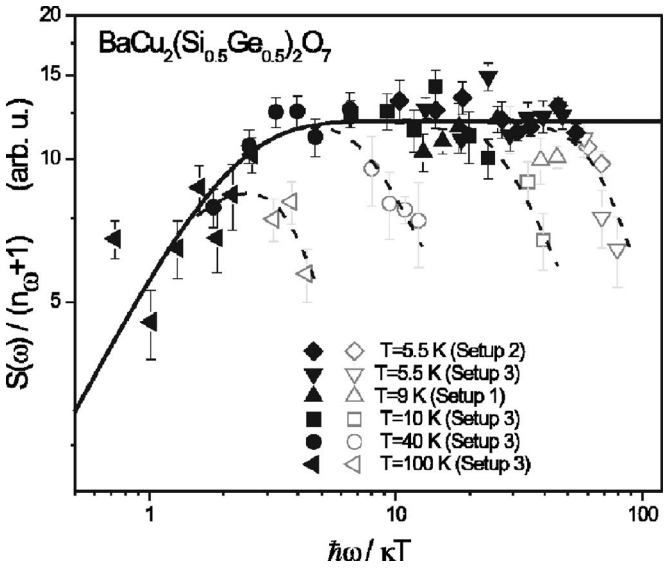

FIG. 7. Measured temperature scaling of $S(\omega)/(n_\omega+1)$ for $BaCu_2(Si_{0.5}Ge_{0.5})_2O_7$. Open symbols correspond to energy transfers above 25 meV. The solid line is the approximate scaling function for a Luttinger spin liquid (Refs. 19 and 24) Dashed lines are guides for the eyes and emphasize the breakdown of scaling at high energies.

taken analytically. However, it can be very accurately approximated by[19,24,25]

$$S(\omega) \sim \tanh\left(\frac{\hbar\omega}{2\kappa T}\right). \tag{3}$$

To a very good approximation, then $S(\omega)=\text{const}$ at $\hbar\omega \gg \kappa T$. The same result can be obtained by integrating the Müller ansatz, which at small $\tilde{q}$ and $\hbar\omega \ll \hbar\omega_{ZB}$ coincides with the $T \to 0$ asymptotic form for the scaling function (2).

The low-temperature data plotted in Fig. 6 show that in $BaCu_2(Si_{0.5}Ge_{0.5})_2O_7$, $S(\omega)$ is indeed practically energy independent up to about 25 meV energy transfer (solid lines), i.e., up to about half of the zone-boundary energy $\hbar\omega_{ZB}$. In this energy range, the measured temperature dependence of $S(\omega)$ is consistent with the scaling form (3), as shown in Fig. 7, solid line. This plot, with a dynamic range for $\hbar\omega/\kappa T$ from 1 to 100, is complementary to that shown in Ref. 19 for Cu benzoate with $\hbar\omega/\kappa T$ in the range of about 0.1–10. Above 25 meV, the measured $S(\omega)$ starts to decrease and $\omega S(\omega)$ deviates from linear behavior, even at low temperatures (Fig. 6, dashed lines). This breakdown of scaling is observed at all temperatures, as shown by the open symbols and dashed lines in Fig. 7.

The observed breakdown of scaling for $S(\omega)$ at about half the zone-boundary energy is rather interesting, if not unexpected. Work on $KCuF_3$ has shown that for $S(\pi,\omega)$, the scaling relation (1) holds at much higher energies, up to about 140% of $\hbar\omega_{ZB}$.[15] Of course, the difference is due to the fact that Eq. (1) is derived for the continuum limit $|\tilde{q}| \ll 1$. Unlike $S(\pi,\omega)$, $S(\omega)$ includes scattering at wave vectors, $-\hbar\omega/v < \tilde{q} < -\hbar\omega/v$, and thus rapidly exceeds the domain of validity of Eq. (1) as $\hbar\omega/v$ increases. Note that the existing $S(\omega)$ scaling data for Cu benzoate also extend to about half of $\hbar\omega_{ZB}$.

V. CONCLUDING REMARKS

It is now clear that at energy transfers exceeding about 0.5 meV, $BaCu_2(Si_{0.5}Ge_{0.5})_2O_7$ behaves as a prototypical disorder-free 1D quantum $S=1/2$ system. In this sense, the claim of Ref. 7 that $BaCu_2(Si_{1-x}Ge_x)_2O_7$ compounds are useful $S=1/2$ chain materials, with a continuously adjustable exchange constant, is fully justified. On the other hand, the suppression of the ordering temperature, the anomalous low-temperature increase in the bulk susceptibility,[6] recent ESR data,[26] and preliminary neutron spin-echo measurements[27] clearly show that at lower energies (longer time scales), quenched disorder *does* become relevant. Understanding the scaling of spin correlations in this regime is a challenge for future studies.

ACKNOWLEDGMENT

Research at ORNL was funded by the United States Department of Energy, Office of Basic Energy Sciences-Materials Science, under Contract No. DE-AC05-00OR22725 with UT-Battelle, LLC.

[1] I. Tsukada, Y. Sasago, K. Uchinokura, A. Zheludev, S. Maslov, G. Shirane, K. Kakurai, and E. Ressouche, Phys. Rev. B **60**, 6601 (1999).
[2] A. Zheludev, S. Raymond, L.-P. Regnault, F. H. L. Essler, K. Kakurai, T. Masuda, and K. Uchinokura, Phys. Rev. B **67**, 134406 (2003).
[3] A. Zheludev, M. Kenzelmann, S. Raymond, T. Masuda, K. Uchinokura, and S.-H. Lee, Phys. Rev. B **65**, 014402 (2001).
[4] A. Zheludev, K. Kakurai, T. Masuda, K. Uchinokura, and K. Nakajima, Phys. Rev. Lett. **89**, 197205 (2002).
[5] A. Zheludev, M. Kenzelmann, S. Raymond, E. Ressouche, T. Masuda, K. Kakurai, S. Maslov, I. Tsukada, K. Uchinokura, and A. Wildes, Phys. Rev. Lett. **85**, 4799 (2000).
[6] T. Masuda, A. Zheludev, K. Uchinokura, J.-H. Chung, and S. Park, Phys. Rev. Lett. **93**, 077206 (2004).
[7] T. Yamada, M. Takano, and Z. Hiroi, J. Alloys Compd. **317–318**, 171 (2001).
[8] T. Yamada, Z. Hiroi, and M. Takano, J. Solid State Chem. **156**, 101 (2001).
[9] C. A. Doty and D. S. Fisher, Phys. Rev. B **45**, 2167 (1992).
[10] C. Dasgupta and S. K. Ma, Phys. Rev. B **22**, 1305 (1980).
[11] K. Damle, O. Motrunich, and D. A. Huse, Phys. Rev. Lett. **84**, 3434 (2000).
[12] O. Motrunich, K. Damle, and D. A. Huse, Phys. Rev. B **63**, 134424 (2001).
[13] T. Masuda, A. Zheludev, K. Uchinokura, J.-H. Chung, and S. Park, Phys. Rev. Lett. **96**, 169908(E) (2006).
[14] D. C. Dender, Ph.D. thesis, Johns Hopkins University, 1997.
[15] B. Lake, D. A. Tennant, C. D. Frost, and S. E. Nagler, Nat. Mater. **4**, 329 (2005).
[16] J. D. Cloizeau and J. J. Pearson, Phys. Rev. **128**, 2131 (1962).
[17] T. Masuda (unpublished).
[18] F. H. L. Essler, A. M. Tsvelik, and G. Delfino, Phys. Rev. B **56**, 11001 (1997).
[19] D. C. Dender, D. Davidovic, D. H. Reich, and C. Broholm, Phys. Rev. B **53**, 2583 (1996).
[20] D. A. Tennant, R. A. Cowley, S. E. Nagler, and A. M. Tsvelik, Phys. Rev. B **52**, 13368 (1995).
[21] D. A. Tennant, S. E. Nagler, D. Welz, G. Shirane, and K. Yamada, Phys. Rev. B **52**, 13381 (1995).
[22] I. A. Zaliznyak, H. Woo, T. G. Perring, C. L. Broholm, C. D. Frost, and H. Takagi, Phys. Rev. Lett. **93**, 087202 (2004).
[23] G. Muller, H. Thomas, M. W. Puga, and H. Beck, J. Phys. C **14**, 3399 (1981).
[24] H. J. Schulz, Phys. Rev. B **34**, 6372 (1986).
[25] O. Starykh, A. W. Sandvik, and R. R. P. Singh, Physica B **241–243**, 563 (1998).
[26] A. I. Smirnov (unpublished).
[27] G. Ehlers, A. Zheludev, and J. Gardener (unpublished).